Published in final edited form as:
Biomaterials. 2010 November ; 31(33): 8706–8715. doi:10.1016/j.biomaterials.2010.07.104.

Neural stem cell adhesion and proliferation on phospholipid bilayers functionalized with RGD peptides

Badriprasad Ananthanarayanan[1,*], **Lauren Little**[2], **David V. Schaffer**[2,3,4], **Kevin E. Healy**[3,5], and **Matthew Tirrell**[1,2,3,5,*]

[1]Department of Chemical Engineering and Materials Research Laboratory, University of California, Santa Barbara, CA 93106

[2]Department of Chemical Engineering, University of California, Berkeley, CA 94720

[3]Department of Bioengineering, University of California, Berkeley, CA 94720

[4]The Helen Wills Neuroscience Institute, University of California, Berkeley, CA 94720

[5]Department of Materials Science and Engineering, University of California, Berkeley, CA 94720

Abstract

Peptide-functionalized materials show promise in controlling stem cell behavior by mimicking cell-matrix interactions. Supported lipid bilayers are an excellent platform for displaying peptides due to their ease of fabrication and low non-specific interactions with cells. In this paper, we report on the behavior of adult hippocampal neural stem cells (NSCs) on phospholipid bilayers functionalized with different RGD-containing peptides: either GGGNGEP**RGD**TYRAY ('bsp-RGD(15)') or G**RGD**SP. Fluid supported bilayers were prepared on glass surfaces by adsorption and fusion of small lipid vesicles incorporating synthetic peptide amphiphiles. NSCs adhered to bilayers with either GRGDSP or bsp-RGD(15) peptide. After 5 days in culture, NSCs formed neurosphere-like aggregates on GRGDSP bilayers, whereas on bsp-RGD(15) bilayers a large fraction of single adhered cells were observed, comparable to monolayer growth seen on laminin controls. NSCs retained their ability to differentiate into neurons and astrocytes on both peptide surfaces. This work illustrates the utility of supported bilayers in displaying peptide ligands and demonstrates that RGD peptides may be useful in synthetic culture systems for stem cells.

Introduction

The stem cell 'niche' refers to the specific microenvironment that regulates the fate of stem cells *in vivo* [1]. The niche controls stem cell fate via soluble signaling molecules, cell-cell interactions with the stromal support tissue, and integrin-mediated cell-matrix interactions with the surrounding extracellular matrix (ECM). A key focus in stem cell engineering is the development of model systems that can control stem cell fate by recapitulating the native microenvironment *in vitro* [2,3]. These model systems are useful for testing hypotheses in stem cell biology as well as for biomedical applications of stem cells. Recreating the stem cell niche requires materials that offer precise control over material architecture and presentation of

[*]Address for correspondence: B.A.: badri@engineering.ucsb.edu, or M.T.: mvtirrell@berkeley.edu.

biological ligands. Several natural, semi-synthetic, and synthetic materials have been investigated for their ability to control cell behavior [4–7], and a common feature in many such synthetic biomaterials is the use of short peptides that mimic the bioactivity of full-length ECM proteins due to their specific recognition by cellular receptors [8].

We have previously reported on the use of supported phospholipid bilayers [9] functionalized with peptide ligands as substrates for integrin-mediated cell adhesion [10,11]. Supported bilayers provide an excellent model surface for these studies for several reasons. In particular, the phospholipid bilayer is a non-fouling surface that resists protein adsorption as well as cell adhesion [12], and can be formed in a facile way by the fusion of small, unilamellar vesicles on glass substrates [13–15]. In addition, we have created bilayer surfaces patterned with peptides via the incorporation of peptide amphiphiles (PAs) – peptides conjugated to hydrophobic 'tail' segments – which self-assemble spontaneously with lipids into vesicles [16]. These self-assembled peptide surfaces can be used to dissect the role of specific ligand-receptor interactions in the adhesion and subsequent behavior of cells. Further, as we have previously demonstrated [11], the lipid bilayer platform is amenable to inclusion of multiple peptides at fixed densities, enabling the rapid creation and screening of surfaces displaying combinations of peptides that may have synergistic effects on cell behavior. Finally, PAs can self-assemble into three-dimensional nanofiber gels that may be useful as scaffolds for stem-cell based tissue engineering applications, since they have been shown to direct neuronal differentiation [7] and promote axon repair in a mouse model of spinal cord injury [17].

Neural stem cells (NSCs) that can proliferate as well as differentiate into all three neural lineages – neurons, astrocytes, and oligodendrocytes – can play an important role in regenerative therapies for diseases such as Alzheimer's disease and Parkinson's disease [18–20]. NSCs are typically propagated in culture on surfaces coated with large ECM proteins such as laminin that can engage several integrin receptors on the cell surface [21]. However, laminin used in cell culture is commonly purified from animal sources, which can introduce batch-to-batch variability as well as the risk of pathogen or immunogen contamination. In an attempt to guide the development of synthetic peptide-based biomaterials that can control stem cell behavior, we investigated whether model bilayer surfaces presenting single peptides at various densities could support the adhesion and proliferation of NSCs. We have previously found that peptides containing the Arg-Gly-Asp (RGD) tri-peptide motif found in several ECM proteins including laminin [22], and known to engage several receptors including β_1 integrins that have been implicated in regulating NSC function *in vivo* [23,24], can support NSC adhesion [25]. Several additional reports have indicated that RGD-containing peptides promote adhesion of NSCs when coupled to polymer surfaces [6,26].

In this study, we used two RGD-containing peptides incorporated in lipid bilayers to probe the effects of differing peptide sequence and surface density on NSC adhesion and proliferation. Further, the ability of the NSCs to proliferate or differentiate on the peptide surfaces in response to soluble factors was assessed by immunofluorescence staining for lineage-specific markers.

Materials and Methods

Materials

The RGD peptides used in this study were: Fmoc-GGGNGEPRGDTYRAY-NH2 ('bsp-RGD (15)', a 15-residue peptide containing the RGD sequence derived from Bone Sialoprotein [27]), and Fmoc-GRGDSP-OH ('GRGDSP', the RGD sequence in Fibronectin [28]). Peptides were obtained on the resin, with all side-groups fully protected, from Anaspec (San Jose, CA). Reagents required for peptide synthesis, including Fmoc-terminated PEG spacers, were obtained from EMD Biosciences (Gibbstown, NJ). Egg yolk phosphatidylcholine ('EggPC') was purchased from Avanti Lipids (Alabaster, AL), and glass-bottom, multi-well plates were

obtained from Mattek (Ashland, MA). Texas Red-conjugated fluorescent lipid TR-DHPE, all fluorophore-conjugated secondary antibodies, the CyQUANT cell proliferation assay kit, N-2 neuronal growth supplement, all cell culture reagents and supplements, polyornithine, and mouse laminin were obtained from Invitrogen (Carlsbad, CA). Recombinant Fibroblast Growth Factor-2 (FGF2) was purchased from Peprotech (Rocky Hill, NJ), Accutase was purchased from Innovative Cell Technologies (San Diego, CA), and retinoic acid was obtained from EMD Biosciences (Gibbstown, NJ). Mouse anti-nestin was purchased from Becton Dickinson (Franklin Lakes, New Jersey), guinea pig anti-glial fibrillary acidic protein (GFAP) from Advanced Immunochemical (Long Beach, CA), and mouse anti-β-tubulin III from Sigma-Aldrich (St. Louis, MO). All other reagents were purchased from Sigma-Aldrich (St. Louis, MO).

Peptide amphiphile synthesis

Peptide amphiphiles were synthesized using an extension of standard Fmoc solid-phase peptide chemistry, as described previously [29]. Briefly, a hydrophobic 'tail' moiety with two 16-carbon alkyl chains was synthesized and conjugated to the N-terminus of the peptide via an intermediate PEG spacer. The crude product obtained after synthesis was purified by reverse-phase high-performance liquid chromatography (RP-HPLC). The peptide mass was verified by Electro-Spray Ionization Mass Spectrometry with Time-of-Flight detection (ESI-MS). The chemical structure of the peptide amphiphiles used in this study is shown in Figure 1(A). The N-terminus of the bsp-RGD(15) peptide was conjugated to a C_{16} di-alkyl tail via a short PEG spacer consisting of two ethylene-oxide units. A longer PEG spacer consisting of five ethylene-oxide units was used to conjugate the GRGDSP peptide to the C_{16} di-alkyl tail. These spacers were chosen based on the peptide sequence and the location of the RGD motif within it to ensure that the RGD group protrudes sufficiently from the self-assembled bilayer surface to be accessible for integrin binding.

Preparation of self-assembled bilayers

Supported phospholipid bilayers incorporating peptide amphiphiles were prepared by vesicle fusion, as described previously [16]. The method is depicted schematically in Figure 1(B). EggPC vesicles incorporating either bsp-RGD(15) or GRGDSP peptide amphiphiles at various mole fractions, as well as 1% TR-DHPE, were first prepared as below. The materials were mixed in the appropriate ratios in a glass vial and dissolved in a common solvent, a chloroform-methanol mixture with a range of 33% v/v. to 75% v/v methanol depending on the PA used and the ratio of PA to EggPC. The solvent was then evaporated under a nitrogen stream to form a thin film, which was further dried under vacuum. The film was re-hydrated at 1 mg/ml in MilliQ water (18.2 MΩ.cm resistivity) at 80 °C with frequent vortexing, to form multi-lamellar vesicles. These were then extruded through a 50 nm pore-size membrane to form small, unilamellar vesicles. The solution of vesicles was further filtered through a disposable 0.22 μm syringe filter to ensure sterility. PA-containing vesicles were stored at 5 °C and used within three weeks of preparation.

For bilayer preparation, sterile glass-bottom multi-well plates (Mattek) or chambered coverslips (Lab-tek II, Fisher Scientific) were used as substrates without any pre-treatment. 8 μl of the vesicle solution was pipetted onto the glass surface in the multi-well plate, and covered with 180 μl of phosphate buffer (10 mM PO_4^{2-}, pH 7.4, 300 mM NaCl). The surface was left undisturbed for 45 min to allow for complete formation of planar bilayers by vesicle fusion. Care was taken to ensure that the bilayer remained fully hydrated during all subsequent handling. The surface was washed twice with sterile PBS to remove all non-adhered vesicles, and then twice with cell culture media (DMEM/F12 with N-2 neuronal growth supplement) in preparation for cell adhesion experiments.

Fluorescence microscopy and FRAP

Supported bilayers incorporating PAs and 1 % mol. TR-DHPE were imaged by fluorescence microscopy. A Nikon Eclipse TE-200 epi-fluorescence microscope equipped with a 100 W mercury arc lamp was used. Images were captured using a Coolsnap ES2 cooled-CCD camera (Photometrics, Tucson, AZ) with QCapture Pro control software (QImaging, Surrey, BC, Canada). Fluorescence images of the bilayer were captured after several PBS wash steps to remove adsorbed vesicles. For Fluorescence Recovery After Photobleaching (FRAP) experiments, the light output from the mercury lamp was sent through a fully stopped-down iris to reduce the field of illumination. The appropriate filter was used for exciting the Texas Red fluorophore and the light was focused through a 100× objective on the bilayer. A spot of roughly 75 μm diameter was bleached for approximately 10 s, following which the fluorescence in the entire field of view was monitored using a 4× objective. Images were taken at 1 min intervals to minimize photobleaching of the bilayer during the recovery process. Image processing and analysis were done using ImageJ software (NIH).

Cell culture and adhesion assays

Neural stem cells (NSCs), previously isolated from the hippocampus of the adult rat brain, were propagated as described [25] on tissue culture plates coated with polyornithine and mouse laminin in serum-free growth media, which consisted of DMEM/F12 supplemented with N-2 and 20 ng/ml FGF2. For cell adhesion assays, cells were removed from the plate using Accutase, aspirated in growth media, and seeded on peptide surfaces at a density of 10,000 cells/cm^2. Laminin-coated tissue-culture plastic surfaces were used as a positive control. Initial cell adhesion was assessed at 2 hours after incubation by inverting the culture plate to remove non-adhered cells. The adhered cells were then fixed using 4% paraformaldehyde in PBS following which the nuclei were stained using DAPI. Fluorescence images were taken at several spots on each surface, and the adhered cells were counted using particle analysis in ImageJ. Longer-term proliferation was assessed by allowing cells to grow on the surfaces for 5 days, with media replacement every 2 days. After 5 days the plates were inverted and washed with PBS. Cell number was determined using the CyQUANT fluorescent dye according to the manufacturer's instructions, using a concurrently measured standard curve to convert fluorescence to cell number.

Immunofluorescence staining

The ability of the NSCs to proliferate or differentiate into mature neural cells was assayed by immunofluorescence staining. NSCs were seeded on test surfaces in DMEM/F12 media with N-2 supplement and either 20 ng/ml FGF2 (growth media) or 0.75% fetal bovine serum (FBS) with 1 μM retinoic acid (mixed differentiation media). After 5 days, the cells were fixed as described above, permeabilized using 0.3% Triton X-100 in PBS, and blocked using 5% goat serum in PBS. Cells grown in proliferative conditions were stained using mouse anti-nestin (1:250), while those grown in mixed differentiating conditions were stained using mouse anti-β-tubulin III at a 1:250 dilution and guinea pig anti-GFAP at a 1:1000 dilution. Detection of primary antibodies was performed with goat secondary antibodies conjugated to Alexa Fluor 488 (anti-nestin and anti-β-tubulin III) or Cy5 (anti-GFAP), used at a 1:250 dilution. Cell nuclei were stained with DAPI.

Data analysis and statistics

Cell adhesion data were obtained from two or more independent experiments, each done in triplicate. Data are shown as mean ± standard error (SEM). Data that are not in the same group (where discrete groups are indicated on graphs by the lowercase letters a, b, etc.) were found to be statistically different ($p < 0.05$) using one-way ANOVA with the Tukey-Kramer MSD post-hoc test.

Results

Vesicle fusion and bilayer characterization

Our strategy for creating ligand-functionalized surfaces is shown schematically in Figure 1(B). RGD-containing peptide amphiphiles (chemical structures shown in Figure 1(A)) were incorporated in EggPC vesicles, following which vesicle adsorption and rupture onto glass surfaces resulted in the formation of peptide-functionalized surfaces [15, 16]. The highest mole fraction of bsp-RGD(15) peptide amphiphile that could be incorporated into lipid vesicles, and therefore on the surface, was found to be 20%. At higher fractions of bsp-RGD(15), the lipid solution formed small, presumably micellar aggregates upon hydration (data not shown). Vesicles containing up to 40% GRGDSP peptide could be formed before micellar aggregates formed instead of lamellar vesicles.

Supported bilayers formed on glass-bottom multi-well plates, with 1% TR-DHPE fluorescent lipid included in the lipid mixture, were imaged by fluorescence microscopy, as shown in Figure 2(A). Pure EggPC bilayers as well as bilayers containing 20% GRGDSP in EggPC showed smooth and uniform fluorescence. Since there are very few fluorescent vesicles in solution due to extensive wash steps performed after bilayer formation, the smooth fluorescence is indicative of the presence of a uniform layer on the surface. Several bright specks of fluorescence are seen, which correspond to vesicles adsorbed to the bilayer surface despite the wash steps. Similar results were obtained with surfaces containing 5% – 40% GRGDSP peptide or 5% – 20% bsp-RGD(15) peptide (data not shown).

To further verify that the surface-associated fluorescence was due to a planar bilayer and not a layer of adsorbed vesicles, Fluorescence Recovery After Photobleaching (FRAP) experiments were performed. In this experiment, the recovery of fluorescence as unbleached fluorophores diffuse into the bleached spot indicates the presence of a fluid bilayer [30,31]. A FRAP image sequence on a 20% GRGDSP bilayer is shown in Figure 2(B), where the fluorescence intensity of a spot (approx. 75 μm diameter) is shown over time. The intensity increased significantly after 15 min, with complete recovery at longer times (data not shown). Similar results were obtained with other surface compositions. Taken together, the fluorescence and FRAP data evidence the formation of fairly uniform fluid supported bilayers displaying peptide amphiphile ligands on the glass surface.

Initial cell adhesion on peptide surfaces

NSCs were incubated on RGD-functionalized bilayers in growth media for a period of 2 hours to determine the extent of initial cell adhesion. This time point was chosen to allow NSCs to adhere while minimizing adsorption of endogenous matrix proteins secreted by the cells, which might mediate cell-surface interactions at longer times and complicate the interpretation of adhesion data. We also note that while the media did contain FGF2 to maintain the cells in the undifferentiated state, it did not contain serum or any other adhesion proteins. EggPC bilayers and tissue-culture treated polystyrene surfaces coated with laminin were used as negative and positive controls, respectively.

The number of cells adhered per unit area on the bilayers with the highest attainable densities of the two RGD peptides, as compared to controls, is shown in Figure 3(A), with phase contrast images of the adhered cells shown in Figure 3(B). NSCs adhered to a very small extent on EggPC bilayer surfaces. Significantly higher cell adhesion was observed on 20% bsp-RGD (15), 40% GRGDSP, and laminin-coated surfaces. Cell adhesion on 20% bsp-RGD(15) surfaces and that on laminin-coated surfaces were not statistically different ($p > 0.05$).

Next, the dependence of NSC adhesion on the surface peptide density was investigated. Bilayer surfaces with varying peptide density were prepared by vesicle fusion. As shown in Figure 4,

NSC adhesion increased with increasing surface density of the bsp-RGD(15) peptide, whereas for the GRGDSP peptide, the extent of adhesion was high at 10% and 40% but lower at an intermediate surface density.

Proliferation on peptide surfaces

In order to determine whether RGD peptide-functionalized surfaces can support longer-term NSC culture, proliferation of NSCs over a period of 5 days was studied. NSCs were cultured in complete growth medium, which contains 20 ng/ml FGF2, a factor known to maintain NSCs in the undifferentiated state [18]. After 5 days, the number of cells on the surfaces was estimated using the CyQUANT assay, and cells were also stained by immunofluorescence for Nestin, an intermediate filament protein selectively expressed in the neural progenitor state [32].

Cells proliferated on all surfaces tested, with significantly higher cell numbers on laminin surfaces compared to peptide surfaces (Figure 5). Cell numbers increased significantly relative to the number of cells that initially adhered (Figure 3), but were statistically indistinguishable on control EggPC surfaces, 20% bsp-RGD(15), and 40% GRGDSP surfaces, which is due to the contribution from cell-cell adhesions and aggregate formation, as detailed below. In addition, Nestin expression was observed on all surfaces tested, as shown in the immunofluorescence images in Figure 6. This verifies that the NSCs were undergoing proliferation in an immature state, as expected in FGF2-containing media. Despite similarities in the total cell numbers and Nestin expression, there were marked differences in the morphology of the adhered cells on bilayer surfaces. NSCs on laminin were found to attach and proliferate essentially as single cells, forming a fairly uniform monolayer (Figure 6). However, on EggPC and 40% GRGDSP surfaces, large aggregates of cells attached to the surface were found, similar to behavior observed on uncoated glass surfaces (data not shown) and to NSC growth in suspension as neurospheres, which are free-floating aggregates that a variety of neural progenitor cells form upon detachment from the substrate. Interestingly, NSCs on 20% bsp-RGD(15) surfaces were found to exhibit behavior intermediate between that on laminin and EggPC surfaces – a significant fraction of singly adhered cells were found, as well as a small number of loose aggregates that were not as large or cohesive as on EggPC or 40% GRGDSP.

Differentiation on peptide surfaces

Previous work has established that in the presence of 0.75% FBS and 1 μM retinoic acid (‘mixed differentiating conditions’), the NSCs used in this work differentiate into an admixture of neurons and astrocytes [25]. In order to determine whether NSCs cultured on RGD-functionalized surfaces retained their hallmark ability to generate mature differentiated cells, NSCs were grown in mixed differentiating conditions for 5 days and stained for lineage-specific markers by immunofluorescence. In addition to cellular morphology, neurons can be identified by expression of β-tubulin III [33] and astrocytes by expression of GFAP [34].

Phase contrast and immunofluorescence images of differentiated cells are shown in Figure 7. The low cell density is due to the absence of the mitogen FGF2 and the presence of factors that halt the cell cycle and induce differentiation. Cells did not adhere strongly to EggPC bilayers under these conditions, resulting in aggregates that could not be assayed for differentiation markers, and very few differentiated cells were thus observed on EggPC surfaces. In contrast, on the peptide surfaces as well as on laminin, cells displaying neuronal morphology and high β-tubulin III expression (shown in green) and cells displaying astrocytic morphology and high GFAP expression (shown in red) were seen. Although image analysis revealed differences in the levels of expression of these markers (data not shown), there were no systematic differences in the number of neuronal and astrocytic cells found on the different surfaces. The fate of the NSCs on the peptide surfaces, as on laminin, was controlled primarily by the media conditions.

Discussion

Phospholipid bilayers displaying RGD peptides at various densities were prepared by vesicle fusion and assayed for NSC adhesion. The fusion process takes less than an hour for completion, and the vesicles, once prepared, can be used without degradation for 2–3 weeks. This process is therefore an extremely facile means to create peptide-functionalized surfaces. The maximum density of peptide on the surface was limited by a vesicle-to-micelle transition at higher ratios of PA to lipid, with the difference between the two peptide amphiphiles due to the larger size of the hydrophilic moiety in the bsp-RGD(15) PA [35]. Nevertheless, the achievable surface densities were high enough to promote NSC adhesion, as shown in Figure 3. The actual surface density of peptide on the bilayer at a given mole fraction can be estimated by making the following assumptions: one, that the molecular area occupied by each peptide head-group is approximately equal to the average phospholipid area in EggPC bilayers, which has been reported to be 70 $Å^2$ [36]; and two, that the PA molecules are equally distributed on both bilayer leaflets. The latter statement holds well for the bilayer of the vesicle, since there is no preferred leaflet in a vesicle membrane with low curvature. Once the supported bilayer is formed from the vesicle, we expect that the original distribution would be retained over the time taken to promote initial cell adhesion, due to the slow rates of lipid flip-flop in a bilayer membrane [37]. Under these assumptions, we estimate the peptide surface density on a 20% bsp-RGD(15) bilayer to be approximately 47 pmol/cm^2. NSC adhesion and proliferation on bsp-RGD(15) modified hydrogel surfaces was previously found to require a surface density between 5 and 11 pmol/cm^2, and reach a value comparable to laminin at 21 pmol/cm^2 [25]. The discrepancy between these results is possibly due to the fact that the EggPC bilayers used in this study are fluid, as evidenced by the FRAP images shown in Figure 2(B), unlike peptides covalently immobilized to a polymeric surface. Freely diffusing PAs in the bilayer may be incapable of resisting integrin-mediated cytoskeletal tension and therefore prevent the formation of strong integrin-ligand bonds. A higher ligand density would then be required to achieve stable cell adhesion. It has previously been observed that cell attachment is much lower on RGD-containing fluid lipid monolayers compared to gel-phase lipid monolayers [38], a difference found to be greater for lower affinity ligand (i.e. linear rather than cyclic RGD peptide) for the same cell type. This is consistent with the argument that the cause of decreased cell adhesion on fluid surfaces is the difficulty of forming stable ligand-receptor bonds, which is exacerbated by low ligand affinity.

The dependence of NSC adhesion on GRGDSP density (Figure 4) is not clear. Adhesion was high on 10% and 40% surfaces, and lower at the intermediate density; but these differences were not statistically significant. We believe the linear GRGDSP ligand has lower affinity for NSCs than bsp-RGD(15), which introduces significant variability in the data and obscures the true density-dependence for this peptide. The difference between the two peptides used was even more marked in longer-term NSC proliferation (Figure 6), where cells grown on bsp-RGD(15) exhibited a phenotype that was comparable to laminin controls, consistent with our previous studies [25], whereas GRGDSP promoted a neurosphere-like morphology. We interpret the above result to mean that the 20% bsp-RGD(15) surface promotes a greater degree of cell-surface adhesion than the EggPC or 40% GRGDSP surfaces, on which cell-cell adhesion is favored. NSCs grown as neurospheres exhibit high heterogeneity in their potency [39], due to the inherent variation in concentrations of nutrients and signaling molecules within the multi-cellular aggregate. Further, for scaffold-based tissue engineering applications involving NSCs, surface coatings that promote stable cell-surface attachment and proliferation are essential. Therefore, the bsp-RGD(15) peptide is more promising than GRGDSP for inclusion in self-assembled PA gels and subsequent mechanistic studies on the effect of RGD peptides on NSC behavior in 3D.

The differential NSC response to the two RGD peptides employed is likely due to differences in the number and strength of adhesion events, as well as potentially the integrin receptors that are engaged. These effects could, in turn, be due to sequence-dependent differences in peptide conformation. The bsp-RGD(15) peptide is possibly presented in a looped conformation, which is facilitated by the increased flexibility of the longer peptide backbone compared to GRGDSP, and stabilized by opposite-charge interactions between the Glu (E) and Arg (R) residues flanking the RGD motif in the sequence, i.e. GGGNG***E***P**RGD**TY***R*AY. This hypothesis is supported by the fact that deletion of the flanking Glu and Arg residues from the bsp-RGD(15) sequence resulted in decreased osteoblast adhesion to a polymer-coupled peptide surface, which was rescued upon cyclizing the peptide [40]. Further, we have previously performed molecular dynamics simulations of the bsp-RGD(15) peptide tethered to a solid surface which revealed that the peptide transiently adopts conformations similar to a type II β-turn [41], which are also exhibited by cyclic RGD peptides containing D-amino acids that show high-affinity binding to integrins [42]. Covalently cyclized RGD peptides are known to have greater affinity than linear versions for many integrins, and thereby, are often more effective at promoting cell adhesion [10,11,43]. For instance, a cyclic RGD peptide has previously been observed to support adhesion and proliferation of mouse fetal NSCs [44]. In contrast, we observed that although the linear GRGDSP peptide did promote NSC adhesion, it did not elicit a stably adhered phenotype. This is consistent with previous reports in which only moderate NSC adhesion was observed on surfaces displaying short, linear RGDS peptides that are not likely to adopt looped conformations in solution [6].

In addition to potential differences in adhesion strength or bond number, it is possible that the two peptides recruit different integrins to the cell-surface contacts, which activate different downstream signaling pathways [45]. The attachment of osteoblasts to bsp-RGD(15) peptide surfaces has been shown to be mediated primarily by $\alpha_v\beta_3$ integrin and, to a lesser extent, $\alpha_2\beta_1$ integrin [46]. $\alpha_v\beta_3$ is one of the two integrins that bind bone sialoprotein in nature [47], and is known to bind selectively to cyclic RGD sequences [42], supporting the argument that the activity of bsp-RGD(15) may be due to a looped conformation adopted in solution. By comparison, the linear GRGDSP peptide has a moderate affinity for $\alpha_5\beta_1$ and $\alpha_v\beta_3$ integrins [42]. The specific integrins each peptide engages on NSCs would have to be further analyzed before any definite conclusions about integrin involvement can be made. At any rate, our results suggest that longer and possibly looped RGD peptides may be more promising candidates than linear ones as ligands for NSC culture.

Several non-RGD peptides have been reported to promote NSC proliferation or differentiation, such as the laminin-derived PPFLMLLKGSTR [48] and IKVAV [7,49] peptides. However, in previous work from our group, the IKVAV peptide failed to induce adhesion or proliferation of rat hippocampal NSCs when grafted to a polymer surface [25]. Nanofiber gels derived from the self-assembly of a peptide with the sequence $(RADA)_n$ have been reported to support proliferation and differentiation of mouse neural stem cells, especially when functionalized with bone-marrow homing peptides [6]. Nevertheless, it seems unlikely that the complex extracellular milieu that regulates the fate of NSCs *in vivo* will be reproduced effectively by a single peptide: for instance, it is known for some NSCs that proliferation and migration are regulated by distinct β_1 integrin-mediated pathways [23]. Therefore, a combinatorial approach wherein the surface presents a cohort of signaling peptides may be required. This approach is analogous to the use of combinations of ECM proteins for controlling stem cell behavior [50, 51]. There has been some work in developing surfaces that can efficiently present multiple peptides to stem cells [25,52]. The lipid bilayer platform used in this work is suitable and in many ways advantageous for inclusion of multiple peptide ligands at controlled densities [11]. Since bilayers are formed by self-assembly, multi-component surfaces can be prepared by mixing the PAs in the appropriate ratios prior to bilayer formation, without the need for orthogonal chemistries or multiple wash steps. Further, the fluidity of the peptide ligands in

the bilayer may allow for cell-mediated clustering and rearrangement of adhesive contacts [53], thereby mimicking native cell-ECM [54] and cell-cell interactions [55,56] to a greater degree. Finally, peptide combinations discovered through the 2D bilayer platform can be easily translated to 3D self-assembled PA gels, which show great promise as biomimetic scaffold materials in wound repair and regenerative medicine [17,57].

Conclusion

The data presented above provide evidence that RGD peptide-functionalized bilayers support NSC adhesion, proliferation, and differentiation into mature neural cells. A stably adhered NSC phenotype comparable to laminin was only observed on bilayers containing the bsp-RGD(15) peptide, which is likely attributed to its integrin engagement profile and affinities. In addition, our data show that supported bilayers that incorporate peptide amphiphiles represent a useful model system for studying ligand-receptor interactions. Importantly, this system is suitable for screening combinations of peptides that may act synergistically in controlling stem cell function and fate, and can easily be translated to 3D gels that may be useful for regenerative therapies *in vivo*.

Acknowledgments

B.A. and M.T. acknowledge funding support from the U.S. Army Research Office through the Armed Forces Institute of Regenerative Medicine, and partial funding for travel and instrument use from the MRSEC Program of the NSF under award DMR05-20415. D.V.S. and K.E.H. acknowledge funding support from NIH R21DE18044.

References

1. Fuchs E, Tumbar T, Guasch G. Socializing with the neighbors: stem cells and their niche. Cell 2004;116 (6):769–778. [PubMed: 15035980]
2. Lutolf MP, Gilbert PM, Blau HM. Designing materials to direct stem-cell fate. Nature 2009;462(7272): 433–441. [PubMed: 19940913]
3. Little L, Healy KE, Schaffer D. Engineering biomaterials for synthetic neural stem cell microenvironments. Chem Rev 2008;108(5):1787–1796. [PubMed: 18476674]
4. Li YJ, Chung EH, Rodriguez RT, Firpo MT, Healy KE. Hydrogels as artificial matrices for human embryonic stem cell self-renewal. J Biomed Mater Res A 2006;79A(1):1–5. [PubMed: 16741988]
5. Gerecht S, Burdick JA, Ferreira LS, Townsend SA, Langer R, Vunjak-Novakovic G. Hyaluronic acid hydrogel for controlled self-renewal and differentiation of human embryonic stem cells. Proc Natl Acad Sci U S A 2007;104(27):11298–11303. [PubMed: 17581871]
6. Gelain F, Bottai D, Vescovi A, Zhang S. Designer self-assembling peptide nanofiber scaffolds for adult mouse neural stem cell 3-dimensional cultures. PLoS One 2006;1(1):e119. [PubMed: 17205123]
7. Silva GA, Czeisler C, Niece KL, Beniash E, Harrington DA, Kessler JA, et al. Selective differentiation of neural progenitor cells by high-epitope density nanofibers. Science 2004;303(5662):1352–1355. [PubMed: 14739465]
8. Massia SP, Hubbell JA. An RGD spacing of 440nm is sufficient for integrin alpha V beta 3-mediated fibroblast spreading and 140nm for focal contact and stress fiber formation. J Cell Biol 1991;114(5): 1089–1100. [PubMed: 1714913]
9. Sackmann E. Supported membranes: scientific and practical applications. Science 1996;271(5245): 43–48. [PubMed: 8539599]
10. Pakalns T, Haverstick KL, Fields GB, McCarthy JB, Mooradian DL, Tirrell M. Cellular recognition of synthetic peptide amphiphiles in self-assembled monolayer films. Biomaterials 1999;20(23–24): 2265–2279. [PubMed: 10614933]
11. Ochsenhirt SE, Kokkoli E, McCarthy JB, Tirrell M. Effect of RGD secondary structure and the synergy site PHSRN on cell adhesion, spreading and specific integrin engagement. Biomaterials 2006;27(20):3863–3874. [PubMed: 16563498]

12. Andersson AS, Glasmastar K, Sutherland D, Lidberg U, Kasemo B. Cell adhesion on supported lipid bilayers. J Biomed Mater Res A 2003;64A(4):622–629. [PubMed: 12601773]
13. Richter RP, Berat R, Brisson AR. Formation of solid-supported lipid bilayers: an integrated view. Langmuir 2006;22(8):3497–3505. [PubMed: 16584220]
14. Keller CA, Glasmästar K, Zhdanov VP, Kasemo B. Formation of supported membranes from vesicles. Phys Rev Lett 2000;84(23):5443. [PubMed: 10990964]
15. Stroumpoulis D, Parra A, Tirrell M. A kinetic study of vesicle fusion on silicon dioxide surfaces by ellipsometry. AIChE J 2006;52(8):2931–2937.
16. Stroumpoulis D, Zhang HN, Rubalcava L, Gliem J, Tirrell M. Cell adhesion and growth to peptide-patterned supported lipid membranes. Langmuir 2007;23(7):3849–3856. [PubMed: 17335250]
17. Tysseling-Mattiace VM, Sahni V, Niece KL, Birch D, Czeisler C, Fehlings MG, et al. Self-assembling nanofibers inhibit glial scar formation and promote axon elongation after spinal cord injury. J Neurosci 2008;28(14):3814–3823. [PubMed: 18385339]
18. Palmer TD, Takahashi J, Gage FH. The adult rat hippocampus contains primordial neural stem cells. Mol Cell Neurosci 1997;8(6):389–404. [PubMed: 9143557]
19. Gage FH. Mammalian neural stem cells. Science 2000;287(5457):1433–1438. [PubMed: 10688783]
20. Lindvall O, Kokaia Z. Stem cells for the treatment of neurological disorders. Nature 2006;441(7097): 1094–1096. [PubMed: 16810245]
21. Powell SK, Kleinman HK. Neuronal laminins and their cellular receptors. Int J Biochem Cell Biol 1997;29(3):401–414. [PubMed: 9202420]
22. Ruoslahti E. RGD and other recognition sequences for integrins. Annu Rev Cell Dev Biol 1996;12:697–715. [PubMed: 8970741]
23. Jacques TS, Relvas JB, Nishimura S, Pytela R, Edwards GM, Streuli CH, et al. Neural precursor cell chain migration and division are regulated through different beta 1 integrins. Development 1998;125 (16):3167–3177. [PubMed: 9671589]
24. Leone DP, Relvas JB, Campos LS, Hemmi S, Brakebusch C, Fassler R, et al. Regulation of neural progenitor proliferation and survival by beta 1 integrins. J Cell Sci 2005;118(12):2589–2599. [PubMed: 15928047]
25. Saha K, Irwin EF, Kozhukh J, Schaffer DV, Healy KE. Biomimetic interfacial interpenetrating polymer networks control neural stem cell behavior. J Biomed Mater Res A 2007;81A(1):240–249. [PubMed: 17236216]
26. Fischer SE, Liu XY, Mao HQ, Harden JL. Controlling cell adhesion to surfaces via associating bioactive triblock proteins. Biomaterials 2007;28(22):3325–3337. [PubMed: 17459470]
27. Rezania A, Thomas CH, Branger AB, Waters CM, Healy KE. The detachment strength and morphology of bone cells contacting materials modified with a peptide sequence found within bone sialoprotein. J Biomed Mater Res 1997;37(1):9–19. [PubMed: 9335344]
28. Pierschbacher MD, Ruoslahti E. Cell attachment activity of fibronectin can be duplicated by small synthetic fragments of the molecule. Nature 1984;309(5963):30–33. [PubMed: 6325925]
29. Berndt P, Fields GB, Tirrell M. Synthetic lipidation of peptides and amino acids: monolayer structure and properties. J Am Chem Soc 1995;117(37):9515–9522.
30. Axelrod D, Koppel DE, Schlessinger J, Elson E, Webb WW. Mobility measurement by analysis of fluorescence photobleaching recovery kinetics. Biophys J 1976;16(9):1055–1069. [PubMed: 786399]
31. Salafsky J, Groves JT, Boxer SG. Architecture and function of membrane proteins in planar supported bilayers: a study with photosynthetic reaction centers. Biochemistry 1996;35(47):14773–14781. [PubMed: 8942639]
32. Lendahl U, Zimmerman LB, McKay RDG. CNS stem cells express a new class of intermediate filament protein. Cell 1990;60(4):585–595. [PubMed: 1689217]
33. Lee MK, Tuttle JB, Rebhun LI, Cleveland DW, Frankfurter A. The expression and posttranslational modification of a neuron-specific beta-tubulin isotype during chick embryogenesis. Cell Motil Cytoskeleton 1990;17(2):118–132. [PubMed: 2257630]
34. Eng LF. Glial Fibrillary Acidic Protein (GFAP) - the major protein of glial intermediate filaments in differentiated astrocytes. J Neuroimmunol 1985;8(4–6):203–214. [PubMed: 2409105]

35. Kenworthy AK, Simon SA, McIntosh TJ. Structure and phase-behavior of lipid suspensions containing phospholipids with covalently attached poly(ethylene glycol). Biophys J 1995;68(5): 1903–1920. [PubMed: 7612833]
36. Petrache HI, Tristram-Nagle S, Nagle JF. Fluid phase structure of EPC and DMPC bilayers. Chem Phys Lipids 1998;95(1):83–94. [PubMed: 9807810]
37. Wimley WC, Thompson TE. Exchange and flip-flop of dimyristoylphosphatidylcholine in liquid-crystalline, gel, and 2-component, 2-phase large unilamellar vesicles. Biochemistry 1990;29(5): 1296–1303. [PubMed: 2322564]
38. Garcia AS, Dellatore SM, Messersmith PB, Miller WM. Effects of supported lipid monolayer fluidity on the adhesion of hematopoietic progenitor cell lines to fibronectin-derived peptide ligands for alpha 5 beta 1 and alpha 4 beta 1 integrins. Langmuir 2009;25(5):2994–3002. [PubMed: 19437769]
39. Bez A, Corsini E, Curti D, Biggiogera M, Colombo A, Nicosia RF, et al. Neurosphere and neurosphere-forming cells: morphological and ultrastructural characterization. Brain Res 2003;993 (1–2):18–29. [PubMed: 14642827]
40. Harbers GM, Healy KE. The effect of ligand type and density on osteoblast adhesion, proliferation, and matrix mineralization. J Biomed Mater Res A 2005;75A(4):855–869. [PubMed: 16121356]
41. Harbers, GM. Computer-aided biomolecular surface engineering of peptide modified materials [Masters of Science (Biomedical Engineering)]. Evanston, IL: Northwestern University; 1998.
42. Pfaff M, Tangemann K, Muller B, Gurrath M, Muller G, Kessler H, et al. Selective recognition of cyclic RGD peptides of NMR defined conformation by alpha IIb beta 3, alpha V beta 3, and alpha 5 beta 1 integrins. J Biol Chem 1994;269(32):20233–20238. [PubMed: 8051114]
43. Pierschbacher MD, Ruoslahti E. Influence of stereochemistry of the sequence Arg-Gly-Asp-Xaa on binding specificity in cell adhesion. J Biol Chem 1987;262(36):17294–17298. [PubMed: 3693352]
44. Freudenberg U, Hermann A, Welzel PB, Stirl K, Schwarz SC, Grimmer M, et al. A star-PEG-heparin hydrogel platform to aid cell replacement therapies for neurodegenerative diseases. Biomaterials 2009;30(28):5049–5060. [PubMed: 19560816]
45. Giancotti FG, Ruoslahti E. Integrin signaling. Science 1999;285(5430):1028–1033. [PubMed: 10446041]
46. Rezania A, Healy KE. Integrin subunits responsible for adhesion of human osteoblast-like cells to biomimetic peptide surfaces. J Orthop Res 1999;17(4):615–623. [PubMed: 10459771]
47. Humphries JD, Byron A, Humphries MJ. Integrin ligands at a glance. J Cell Sci 2006;119(19):3901–3903. [PubMed: 16988024]
48. Hiraoka M, Kato K, Nakaji-Hirabayashi T, Iwata H. Enhanced survival of neural cells embedded in hydrogels composed of collagen and laminin-derived cell adhesive peptide. Bioconjug Chem 2009;20(5):976–983. [PubMed: 19351184]
49. Thid D, Holm K, Eriksson PS, Ekeroth J, Kasemo B, Gold J. Supported phospholipid bilayers as a platform for neural progenitor cell culture. J Biomed Mater Res A 2008;84A(4):940–953. [PubMed: 17647234]
50. Nakajima M, Ishimuro T, Kato K, Ko IK, Hirata I, Arima Y, et al. Combinatorial protein display for the cell-based screening of biomaterials that direct neural stem cell differentiation. Biomaterials 2007;28(6):1048–1060. [PubMed: 17081602]
51. Flaim CJ, Chien S, Bhatia SN. An extracellular matrix microarray for probing cellular differentiation. Nat Methods 2005;2(2):119–125. [PubMed: 15782209]
52. Derda R, Li LY, Orner BP, Lewis RL, Thomson JA, Kiessling LL. Defined substrates for human embryonic stem cell growth identified from surface arrays. ACS Chem Biol 2007;2(5):347–355. [PubMed: 17480050]
53. Marchi-Artzner V, Lorz B, Gosse C, Jullien L, Merkel R, Kessler H, et al. Adhesion of Arg-Gly-Asp (RGD) peptide vesicles onto an integrin surface: visualization of the segregation of RGD ligands into the adhesion plaques by fluorescence. Langmuir 2003;19(3):835–841.
54. Berrier AL, Yamada KM. Cell-matrix adhesion. J Cell Physiol 2007;213(3):565–573. [PubMed: 17680633]
55. Chan PY, Lawrence MB, Dustin ML, Ferguson LM, Golan DE, Springer TA. Influence of receptor lateral mobility on adhesion strengthening between membranes containing LFA-3 and CD2. J Cell Biol 1991;115(1):245–255. [PubMed: 1717480]

56. Perez TD, Nelson WJ, Boxer SG, Kam L. E-cadherin tethered to micropatterned supported lipid bilayers as a model for cell adhesion. Langmuir 2005;21(25):11963–11968. [PubMed: 16316139]

57. Ellis-Behnke RG, Liang YX, You SW, Tay DKC, Zhang SG, So KF, et al. Nano neuro knitting: peptide nanofiber scaffold for brain repair and axon regeneration with functional return of vision. Proc Natl Acad Sci U S A 2006;103(13):5054–5059. [PubMed: 16549776]

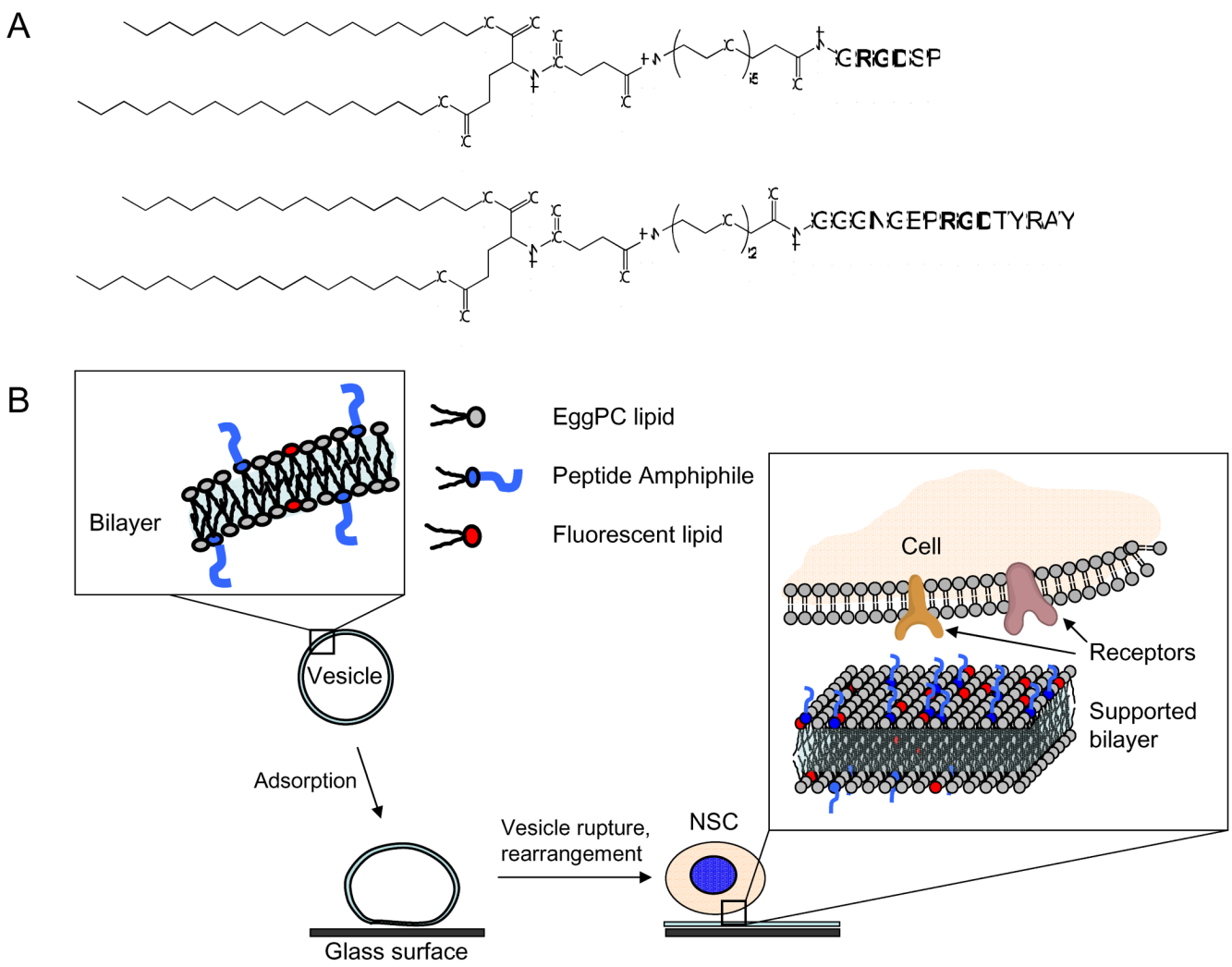

Figure 1.

(A) Chemical structures of the peptide amphiphiles used in this study. **(B)** Schematic representation of the method used to create peptide-functionalized surfaces for studying adhesion of neural stem cells (not drawn to scale).

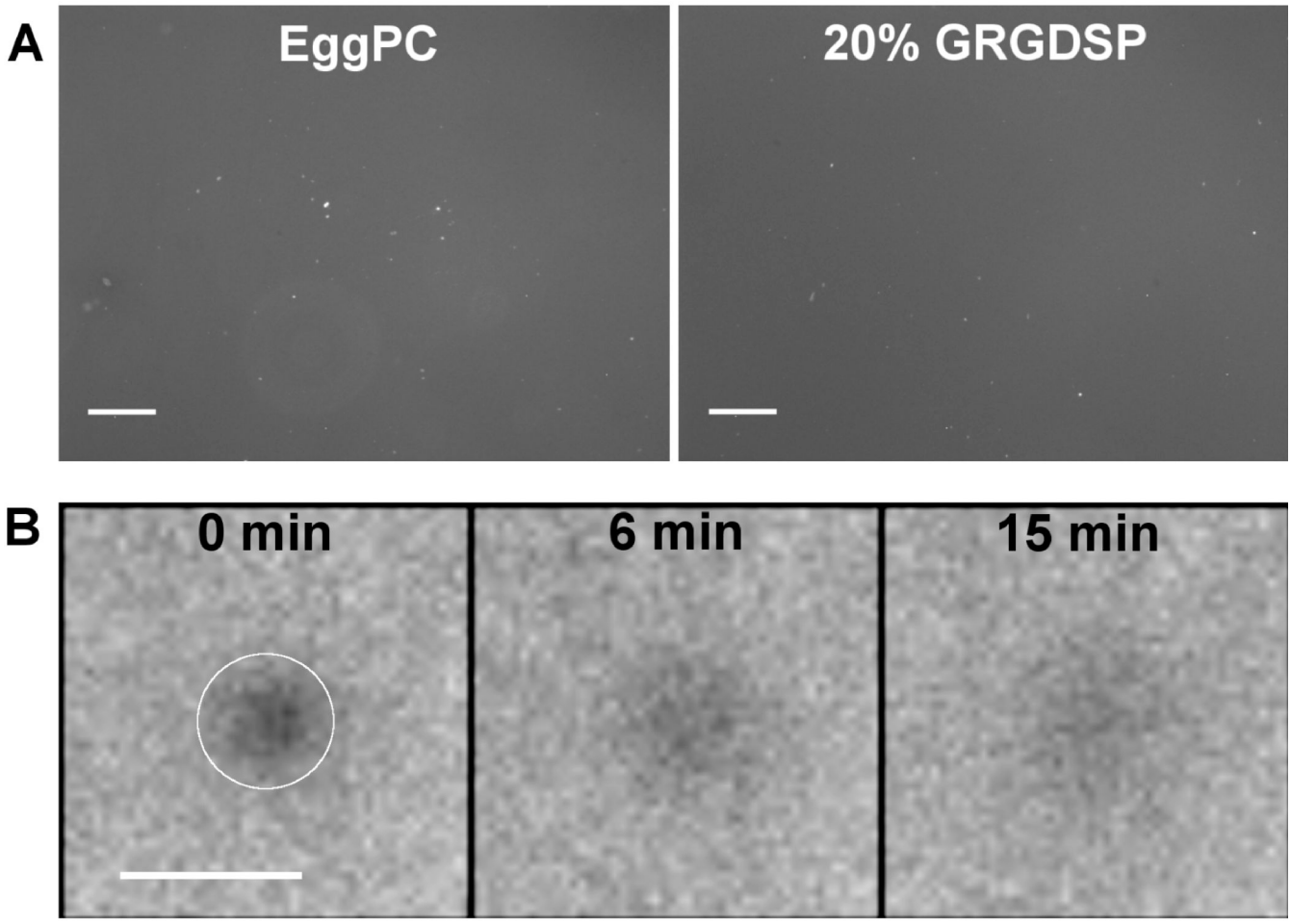

Figure 2.

(A) Fluorescence microscopy images of bilayers formed by vesicle fusion, where 1% TR-DHPE lipid was included in the lipid mixture. Smooth and uniform fluorescence was observed for pure EggPC as well as RGD peptide-containing bilayers. Scale bar: 250 μm. **(B)** Fluorescence recovery after photobleaching (FRAP) image sequence of a photobleached spot (indicated by the white circle) on a 20% GRGDSP bilayer. Fluorescence intensity in the spot increased significantly 15 min after bleaching, verifying the formation of a fluid supported bilayer. Scale bar: 100 μm.

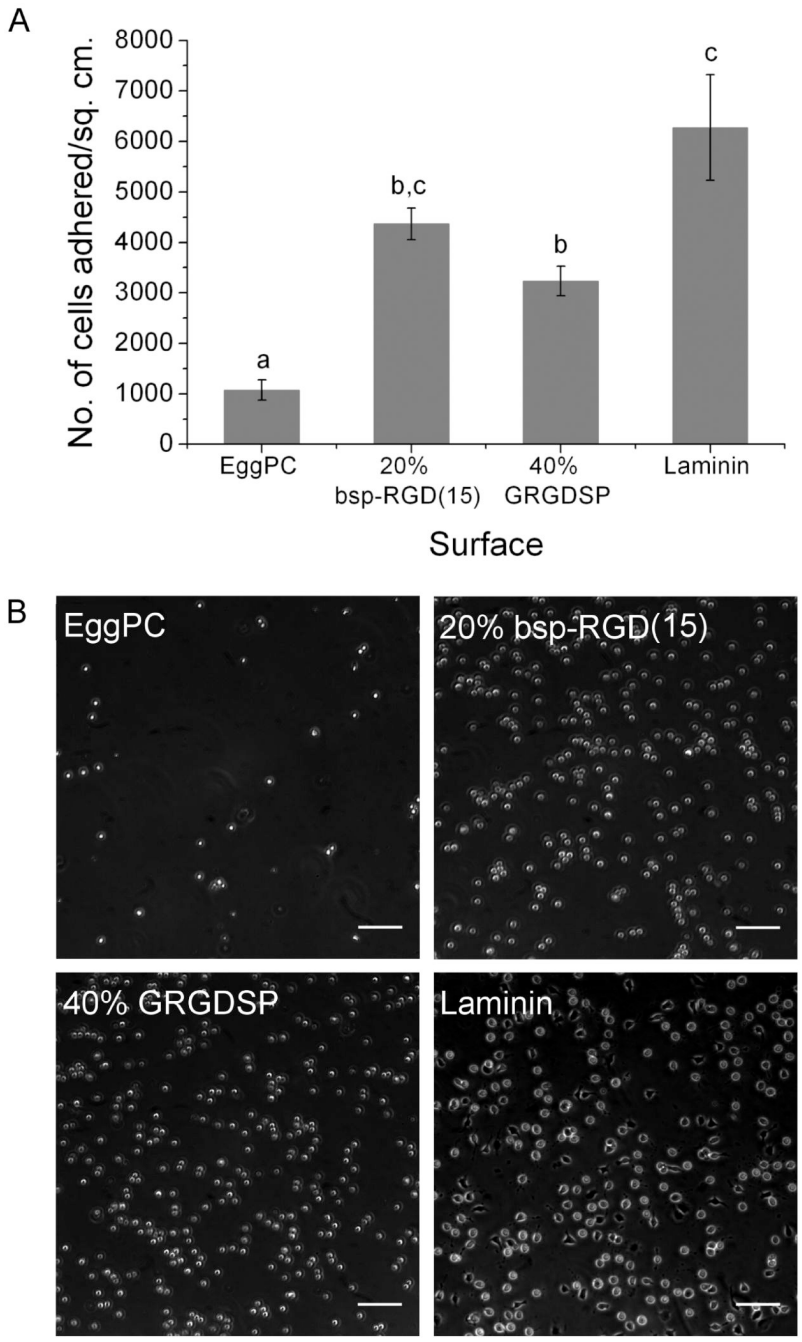

Figure 3.

Neural stem cell adhesion on surfaces after 2 h incubation. **(A)** Number of cells adhered per unit area, as determined by counting DAPI-stained nuclei. Bars show mean ± SEM ($n \geq 6$). Adhesion on 20% bsp-RGD(15) and 40% GRGDSP surfaces was significantly greater than EggPC control; with adhesion on 20% bsp-RGD(15) being comparable to that on laminin. **(B)** Phase contrast images of adhered cells. Scale bar: 100 μm.

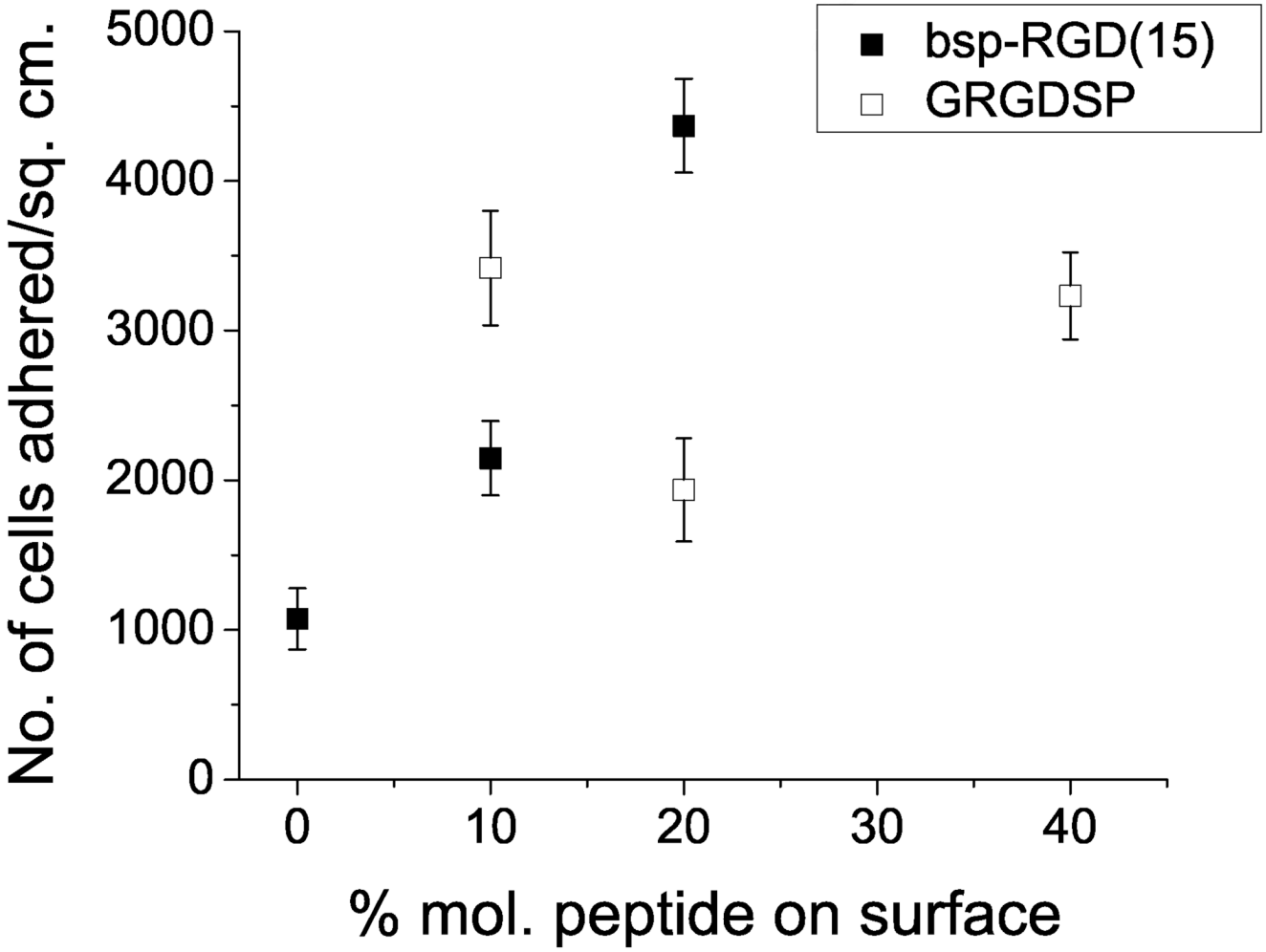

Figure 4.

Neural stem cell adhesion as a function of the molar ratio of peptides incorporated in the EggPC bilayer. Data points show mean ± SEM ($n \geq 6$). Adhesion increased with increasing density of bsp-RGD(15) peptide. For the GRGDSP peptide, adhesion was high at 10% and 40% but lower at 20%.

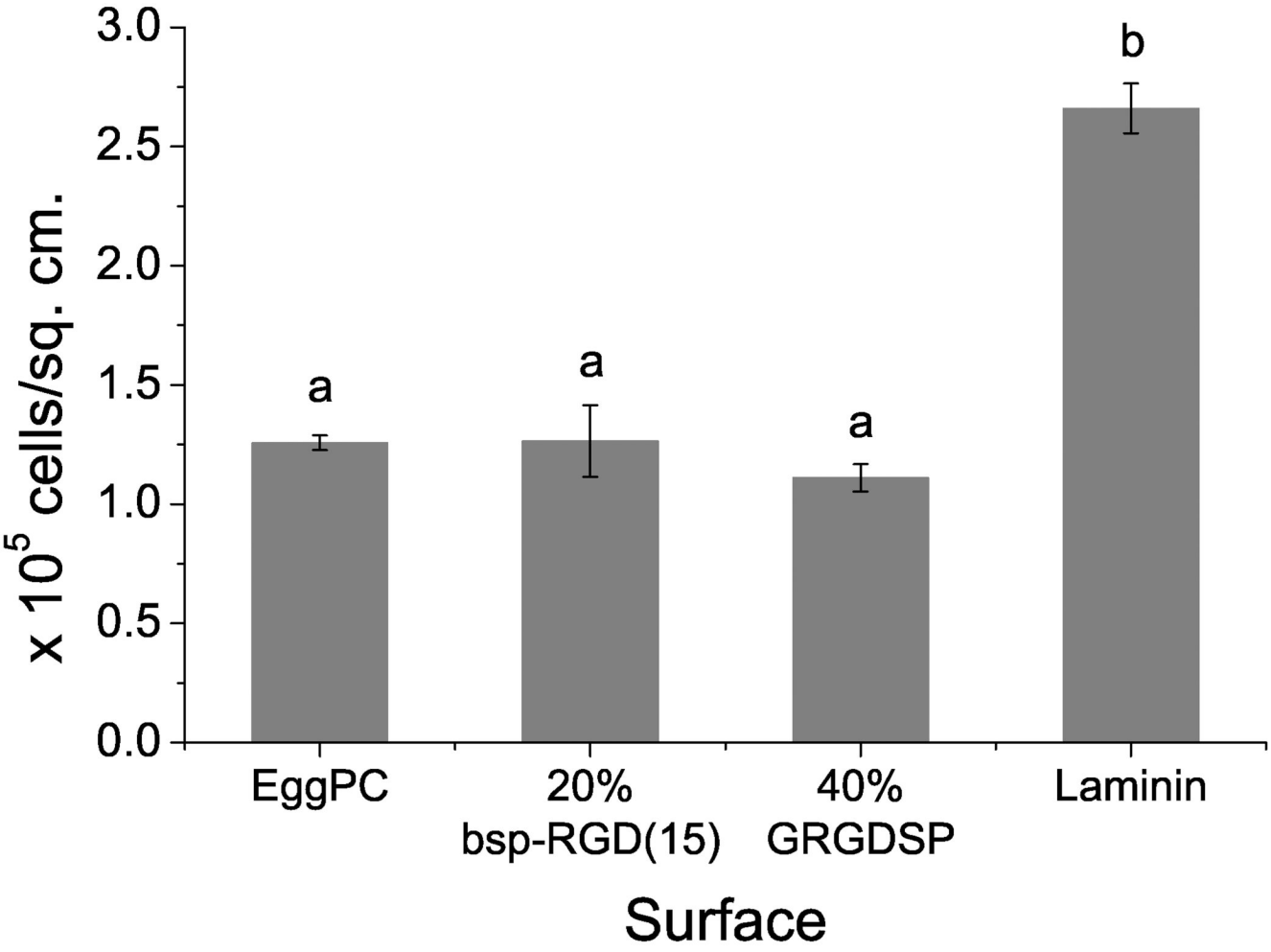

Figure 5.
NSC proliferation after incubation in growth media for 5 days, as determined by cell counts using the CyQUANT assay. Bars show mean ± SEM ($n \geq 3$).NSCs proliferated on all surfaces, but cell numbers on laminin were significantly greater than on other surfaces.

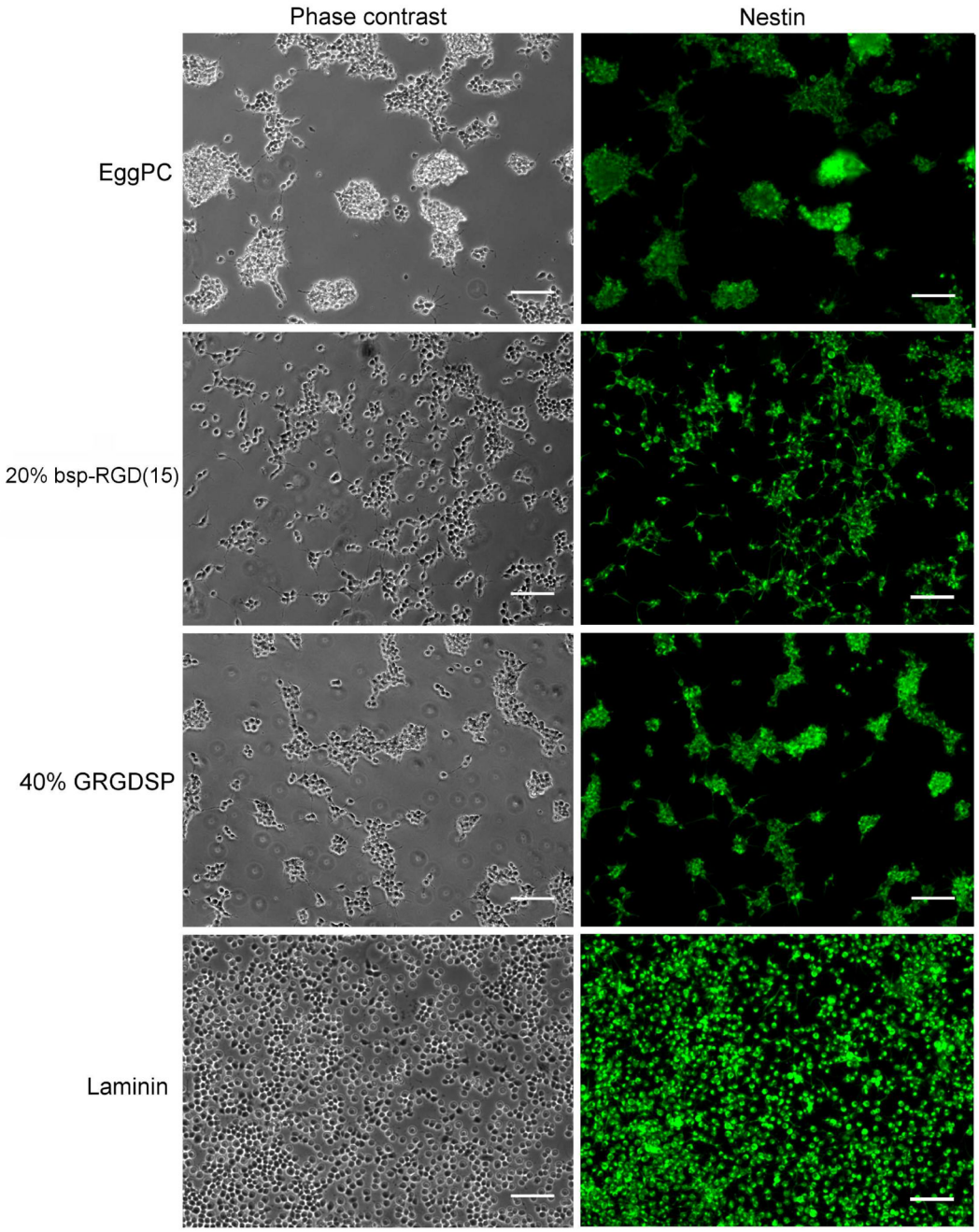

Figure 6.
Phase contrast and immunofluorescence images of NSCs after incubation in FGF2-containing media for 5 days. NSCs grown on all surfaces proliferated and expressed Nestin (shown in green). Cells on EggPC and 40% GRGDSP surfaces formed loosely attached aggregates, whereas cells on laminin, and to a lesser extent, 20% bsp-RGD(15), grew as a monolayer of single cells attached to the surface. Scale bar: 100 μm.

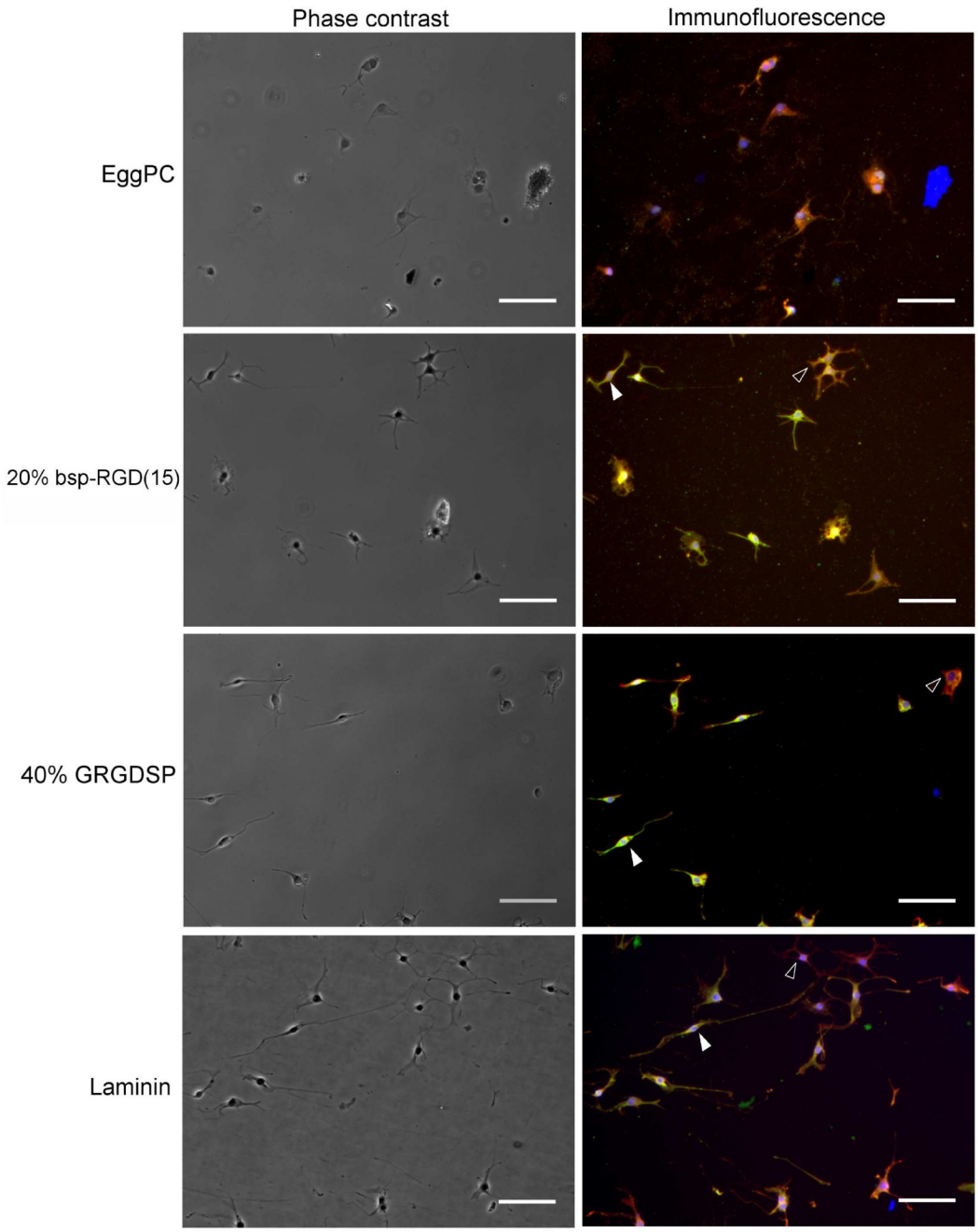

Figure 7.
Phase contrast and immunofluorescence images of NSCs after incubation in mixed differentiating conditions (0.75% FBS and 1 μM forskolin) for 5 days. β-tubulin III expression is shown in green, GFAP in red, and nuclear DAPI staining in blue. NSCs differentiated into an admixture of neuronal cells with high β-tubulin III expression (filled arrowheads) and astrocytes with high GFAP expression (empty arrowheads). Scale bar: 100 μm.